

# Bench2Drive-R: Turning Real World Data into Reactive Closed-Loop Autonomous Driving Benchmark by Generative Model

Junqi You\*

Xiaosong Jia\*

Zhiyuan Zhang

Yutao Zhu

Junchi Yan<sup>†</sup>\* Equal contributions. <sup>†</sup> Correspondence author

Dept. of CSE &amp; School of AI &amp; MoE Key Lab of AI, Shanghai Jiao Tong University

## Abstract

For end-to-end autonomous driving (E2E-AD), the evaluation system remains an open problem. Existing closed-loop evaluation protocols usually rely on simulators like CARLA being less realistic; while NAVSIM using real-world vision data, yet is limited to fixed planning trajectories in short horizon and assumes other agents are not reactive.

We introduce **Bench2Drive-R**, a generative framework that enables reactive closed-loop evaluation. Unlike existing video generative models for AD, the proposed designs are tailored for interactive simulation, where sensor rendering and behavior rollout are decoupled by applying a separate behavioral controller to simulate the reactions of surrounding agents. As a result, the renderer could focus on image fidelity, control adherence, and spatial-temporal coherence. For temporal consistency, due to the step-wise interaction nature of simulation, we design a noise modulating temporal encoder with Gaussian blurring to encourage long-horizon autoregressive rollout of image sequences without deteriorating distribution shifts. For spatial consistency, a retrieval mechanism, which takes the spatially nearest images as references, is introduced to ensure scene-level rendering fidelity during the generation process. The spatial relations between target and reference are explicitly modeled with 3D relative position encodings and the potential over-reliance of reference images is mitigated with hierarchical sampling and classifier-free guidance.

We compare the generation quality of Bench2Drive-R with existing generative models and achieve state-of-the-art performance. We further integrate Bench2Drive-R into nuPlan and evaluate the generative qualities with closed-loop simulation results. We will open source our code.

Table 1. Evaluation Framework for E2E-AD models.

	Sensor Fidelity	Human Behavior	Ego Movement	Reactive
Open-Loop [4]	✓	✓	✗	✗
Simulator [18, 44]	✗	✗	✓	✓
NAVSIM [15]	✓	✓	✓	✗
<b>Bench2Drive-R</b>	✓	✓	✓	✓

## 1. Introduction

End-to-end autonomous driving (E2E-AD) [32, 45, 91] has recently gained pervasive attention from both industry and academia [102]. Unlike traditional modular AD systems, E2E-AD aims to directly predict future trajectories based on raw sensor data. As still in its early stage, benchmarking E2E-AD models remains an open problem. Existing evaluation approaches can be categorized into three classes. (1) **Open-Loop Evaluation** [4] typically measures displacement errors between predicted trajectories and logged expert trajectories. Recent studies [14, 57, 105] reveal that it suffers from imbalanced datasets, heavy reliance on expert ego state, and distribution shift, etc. (2) **Closed-Loop Simulation** [11, 44, 69] utilizes simulators, such as CARLA [18], to evaluate the planning performance in a reactive way. However, there still remain notable gaps between simulator and real world from both rendering and behavioral perspectives. (3) Recent work NAVSIM [15] proposes an intermediate approach situated between open-loop and closed-loop evaluation. It proposes a non-reactive simulator and collects closed-loop evaluation metrics over a short period of simulation horizon. Ego trajectories are predicted at the initial frame and kept fixed during the simulation period. While it can provide realistic sensor images and align more closely with closed-loop metrics than open-loop

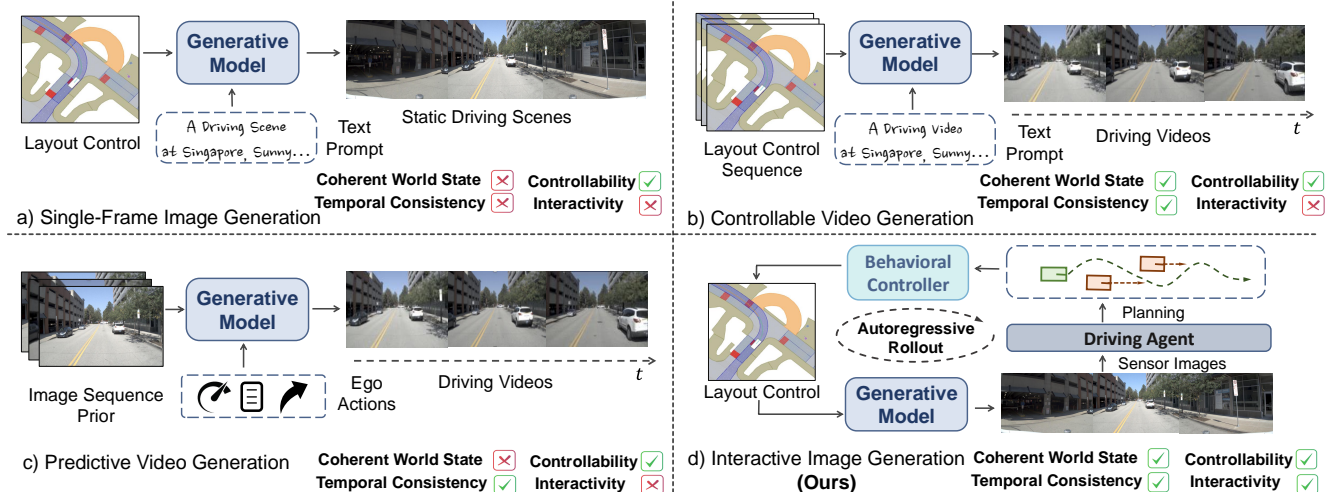


Figure 1. **Different Paradigms of Generative Models for Autonomous Driving:** (a) **Single-Frame Image Generation** [20, 80, 99], as relatively early works, do not account for temporal generation. (b) **Controllable Video Generation** [65, 87, 90] focuses on generating videos with controls for each frame, which is not suitable for interactive simulation. (c) **Predictive Video Generation** [21, 30, 88] emphasizes the annotation-free training ability, which lacks the ability to adhere to control. (d) **Interactive Image Generation:** The proposed framework leverages the power of generative models in an autoregressive manner, enabling high-frequency interactions with end-to-end driving models and generating temporally consistent images. The integration of a rule-based behavioral controller simulates the behavior of other driving agents to ensure a coherent world state and provides layout controls for the generative part of the framework.

displacement errors, it fails to capture the model’s planning capabilities in scenarios where agent interactions [38, 41] critically impact planning outcomes, such as merging into traffic streams or lane changes in dense traffic. We compare different paradigms for E2E-AD evaluation in Table 1.

One promising way to address the aforementioned challenges is to develop a **reactive closed-loop simulation** framework capable of delivering authentic sensor data with high fidelity and consistency. Considerable works have explored the application of generative models to autonomous driving e.g. generating realistic sensor data, most of which have focused on generating novel driving scenes primarily for data augmentation in perception tasks. These efforts include generating static BEV-conditioned driving scenarios for detection and online mapping [20, 80, 99], producing video clips [65, 89, 90] for tasks such as tracking and trajectory prediction, as well as using video diffusion model as world models to implicitly simulate driving scenarios [21, 87, 113]. However, single-frame image generation lacks the constraint of temporal consistency while video generation is not able to conduct step-by-step interactions with E2E-AD models and thus could not be used in the closed-loop interactive simulation. Fig. 1 gives comparison of aforementioned generation paradigms.

To this end, we propose **Bench2Drive-R**, an interactive generative method with autoregressive rollout for closed-loop reactive evaluation for E2E-AD models. Specifically, Bench2Drive-R consists of two parts: **a reactive behav-**

**ioral controller and a generative renderer.** We base our behavioral controller on the widely used planning benchmark -nuPlan [46] while the generative renderer is based on diffusion models [27] with condition controls [108]. At each iteration, E2E-AD models output planned actions based on current sensor data. Then, the reactive behavioral controller takes in this planning results and rollouts driving scenario in the bounding box level (forwarding ego state and other driving agents’ states). Finally, with the new states of environments and previous steps as conditions, the generative renderer produces corresponding sensor data at the updated frame, which is fed into E2E-AD models for next action.

As a **simulation-oriented generative renderer**, several unique characteristics could be utilized for better fidelity and consistency: (1) For **temporal consistency**, the previous frame could always be used as conditions to provide priors. However, it introduces significant train-val gaps which collapse generation easily due to the cumulative errors of autoregressive generation. Thus, we propose a noise modulation module with Gaussian blurring during the training process to let the model adapt to the defective conditions. (2) For **spatial consistency**, our key observation is that **the static background could be retrieved from the database and thus the uncertainty is eliminated.** This point is quite different from video generation models since their purpose is to provide diverse samples while our goal is to provide high-fidelity simulation. Thus, we retrieve the two frames



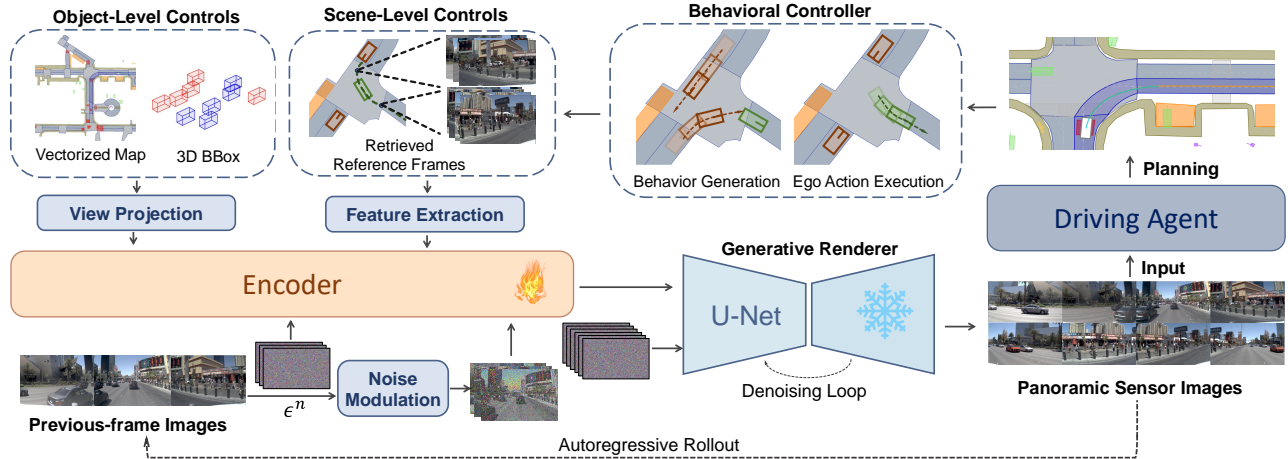


Figure 2. **Overall Framework:** The proposed Bench2Drive-R is composed of two parts: a **behavioral controller** that executes ego actions and generates behaviors of other driving agents; a **generative renderer** that produces multi-view sensor images in an autoregressive manner. To improve fidelity, the generative renderer (1) utilizes previous-frame image for temporal consistency; (2) retrieves spatially nearest reference image pair for background prior; (3) adheres to projected layout element controls for object-level consistency.

with lowest distance in the forward and backward direction respectively and use them as conditions to guide the generation of static background.

We compare the proposed simulation-oriented generative renderer in Bench2Drive-R with state-of-the-art generative models for AD and demonstrate superior fidelity. Further, we implement a closed-loop interactive end-to-end simulation platform based on nuPlan. We compare Bench2Drive-R with baseline generative methods by comparing the performance of the same E2E-AD models under different renderers and Bench2Drive-R demonstrates explicit advantages. We conduct ablation studies and case analysis to evaluate the effectiveness of proposed module.

In summary, our contributions are as follows:

- We introduce **Bench2Drive-R**, the first generative (especially conditioned on real-world driving data), closed-loop reactive simulation framework serving as an end-to-end extension of the planning-only nuPlan.
- Different from the recent efforts [1, 21, 21, 30, 30, 33, 37, 37, 48, 48, 52, 87, 87, 88, 88–90, 94, 113, 113] of video generation, we propose several simulation-oriented designs, which significantly enhance the generation fidelity.
- Extensive experiments including ablation studies on the nuScenes and nuPlan dataset show the effectiveness of the whole proposed framework as well as each module.

## 2. Related Works

### 2.1. Benchmarks for End-to-End Driving Models

E2E-AD methods transform the entire AD system into a learnable network to directly optimize the planning performance. Over the years, E2E-AD has gradually developed

from taking only simulated sensor data [5, 6, 10, 12, 13, 29, 36, 42, 68, 69, 71, 75, 76, 92, 109, 111] to training on real-world collected data [31, 32, 45, 54, 56, 78, 79, 91, 106, 110]. Many existing E2E models are evaluated on the open-loop nuScenes protocol [4], where the displacement errors between expert and predicted trajectories are used as metrics. However, open-loop evaluation has significant limitations, as pointed out in [14, 57, 105]. As for the closed-loop benchmarks, CARLA [18]’s simulation has large gaps compared to real world in both rendering and behavior level while Waymax [22] and nuPlan [46] are limited to bounding box level assessments. Recently, NAVSIM [15] workarounds the problem by introducing an open-loop metric PDMS which shows better correlation to close-loop metrics than displacement errors. However, NAVSIM assumes other vehicles are not reactive and fixes the ego vehicle’s behavior in the simulation period, which cannot reflect the driving performance under highly interactive scenarios.

In this work, we aim to build a closed-loop interactive end-to-end driving simulation, leveraging the recent huge advance in generative models.

### 2.2. Generative and Restriction Models for AD

Diffusion models [27, 77] generate image by progressively denoising a randomly sampled Gaussian noise. Recent advances in the field has allowed diffusion models to generate photorealistic synthesis of images conditioned on various input including text prompts, images, etc. [53, 66, 108]

In the field of autonomous driving, many works try to synthesize novel street-view with generative models. A line of works focus on using generated images as data argumentation for downstream perception tasks. Some

works [20, 80, 96, 99, 107, 117] use bounding boxes and map polylines as controls to generate single-frame driving scene. Other works have advanced into the area of layout controlled video generation with high temporal consistency [1, 17, 24, 24, 33, 52, 58, 89, 90, 94, 95] and explore the impact of synthesized data on detection [50, 118] and prediction [39, 40, 43] tasks.

Another line of works [21, 30, 37, 48, 85, 87, 88, 113] focuses on the predictive capability of generative models. They explore the possibility of turning video diffusion model into generalizable driving world model of a fully differentiable driving simulator, which rollouts world states in pixel space based on input actions and behaviors. However, such world models can't guarantee a coherent world state and fails to provide interactive interfaces for simulations.

Other efforts are spent on closing simulation with reality with 3D reconstruction techniques, such as NeRF [23, 35, 62, 70, 81, 101] and 3D GS [7, 8, 19, 34, 67, 82, 98, 103, 104, 112, 112, 116]. However, reconstruction methods are not fit for simulation task because of their costly reconstructing processes and weak generalizability for out-of-distribution driving cases.

In summary, none of existing works are very suitable for simulation, which motivates us to design simulation oriented Bench2Drive-R, featuring interactive generation. There are also some concurrent works [64, 97, 100, 115] probing into the area of closed-loop simulation with sensor data, but they either resort to spatially-restricted 3D reconstruction methods, which can't provide fine-grind controls, or fail to provide reactive, data-driven [63, 93] traffic simulation.

### 3. Methods

#### 3.1. Preliminaries

**Latent Diffusion Model with Control.** We use latent diffusion model (LDM) [73] as the renderer module. LDM consists of two components: a variational autoencoder (VAE), which compresses input image to latent space with an encoder  $z = E(I)$  and reconstructs latent features to image space with a decoder  $I = D(z)$ , and a 2D U-Net, which is trained by predicting the noise added to latent features at timestep  $t \in (1, 2, \dots, T)$ . Training loss for LDM is:

$$\mathcal{L}_{\text{LDM}} = \mathbb{E}_{\epsilon_t \in \mathcal{N}(0,1), t \in \mathcal{U}[0,T], c} [ \|\epsilon_t - \epsilon_\theta(z_t; t, c)\|^2 ] \quad (1)$$

where  $z_t$  is the noisy latent at timestep  $t$ ,  $\epsilon_\theta$  is the noise prediction network to be trained,  $c$  is the control for conditional generation. During inference, LDM generates images by iteratively removing U-Net-predicted noise from randomly sampled Gaussian noise for  $T$  steps. For fair comparisons with existing works [20], we adopt the pretrained Stable Diffusion v1.5 as our base LDM.

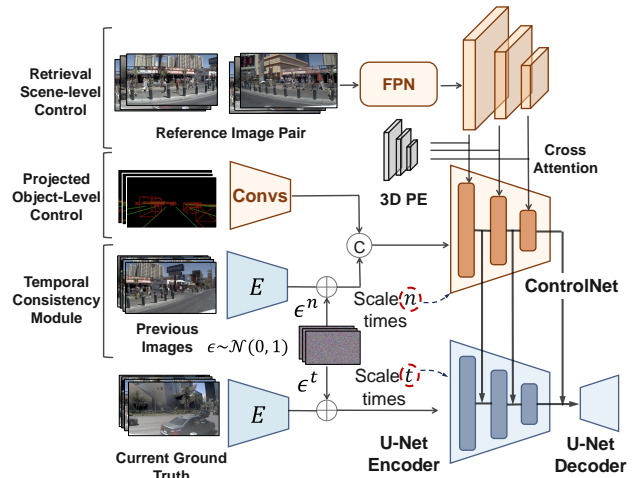


Figure 3. **Structural Design of Generative Renderer.** We design three additive modules to ensure controllable, consistent, and interactive image generation. **a) Temporal consistency module** incorporates previous frame images. Noise modulation module helps prevent distribution drift during autoregressive rollout. **b) Projected Object-Level Control** allows fine-grind controls over the location and orientation of driving vehicles in the scenario. **c) Retrieval Scene-Level Control** ensures spatial consistency by extracting multi-level features from nearest reference image pairs injecting them into the ControlNet with attention mechanism.

Aside from using text prompt guidance in the original LDM, Bench2Drive-R also incorporates pixel-space guidance using ControlNet [108]. ControlNet creates a trainable copy of the U-Net encoder. The outputs from each layer of the ControlNet are added to the outputs of the corresponding layer in the original U-Net encoders. ControlNet and U-Net are connected via zero-conv module to prevent random noise at the early stage of training.

**nuPlan Simulator and Benchmark.** nuPlan [46] is a widely used reactive closed-loop planning benchmark based on large-scale real world data. nuPlan divides a long real-world driving journey into smaller, manageable driving scenarios. Each scenario has high-level navigation information such as goal points and route plans. It also contains sensor data collected along expert trajectories.

#### 3.2. Overall Framework

In Bench2Drive-R, we base our behavioral controller on nuPlan simulator [46], which keeps track of all the structural information of a driving scenario. At a given time  $t$ , the simulator is able to provide the following information:

- 3D bounding boxes and semantic labels:**  $\mathbf{B}_t = \{(b_i, c_i)\}_{i=1}^{N_b}$ , where  $b_i = (x_j, y_j, z_j)_{j=1}^3 \in \mathbb{R}^{8 \times 3}$  is the bounding boxes for both dynamic and static objects (cars, pedestrians, obstacles, etc.) within a specific range;  $c_i \in \mathcal{C}_{box}$  is the semantic label.

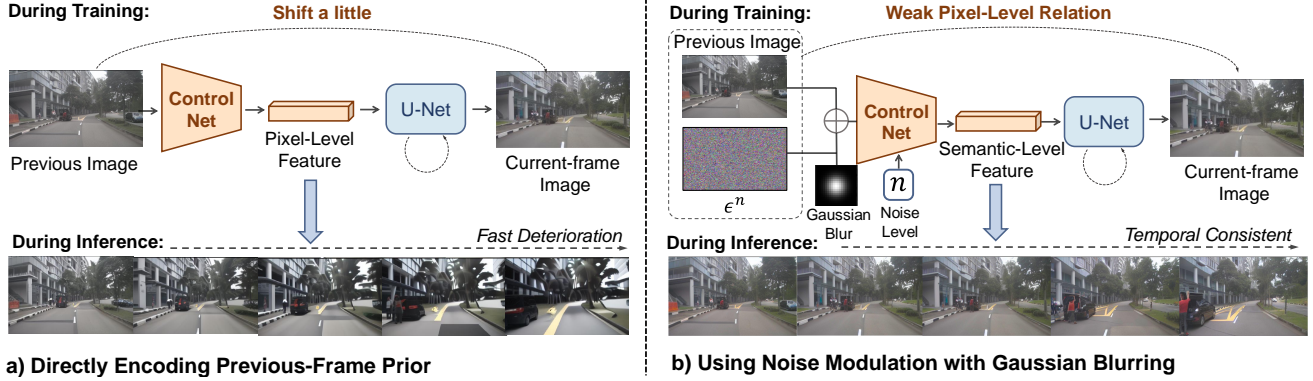


Figure 4. **Deal with Autoregressive Distribution Shift.** **a)** During training, due to the resemblance between previous and current frame prior, the model would overly rely on previous frame. During inference, the generation errors (artifacts) will cumulate and finally collapse. **b)** Adding Gaussian blurring and a random level of noise to previous images can destroy obvious pixel-level relations between the two frames. Noise level  $n$  is fed as inputs to give model hints on the corrupted extent. As a result, the model can adapt to degenerated previous images and learn to extract high-level prior information instead of pixel-level copy.

2. **Vectorized map elements:**  $\mathbf{M}_t = \{(v_i, c_i)\}_{i=1}^{N_m}$ , where  $v_i = (x_j, y_j)_{j=1}^{N_v}$  represents vertices for polygon map elements (roadblocks, cross-walk regions, etc.) and interior points for linestring map elements (lane dividers, stop lines, etc.);  $c_i \in \mathcal{C}_{map}$  represents the map class.
3. **Ego states:**  $\mathbf{E}_t \in \mathbb{R}^{N_e}$ , including ego velocity, acceleration, steering angle, ego-to-global matrix etc.
4. **Camera parameters:**  $\mathbf{K} = \{\mathbf{K}_i \in \mathbb{R}^{4 \times 4}\}_{i=1}^{N_{cam}}$ , where  $\mathbf{K}_i$  is the camera transformation matrix composed of intrinsic and extrinsic matrices that transforms points from Lidar coordinate system to image coordinate system.
5. **Original recorded sensor images with global ego coordinates:**  $\{(\text{coord}_i, \mathbf{I}_i)\}_{i=1}^{N_f}$ , where  $N_f$  is the number of total frames in current scenario;  $\text{coord}_i$  is the position of ego vehicle under global coordinate system;  $\mathbf{I}_i^{ref} \in \mathbb{R}^{N_{cam} \times C \times H \times W}$  represents sensor images collected by  $N_{cam}$  cameras. Note that they are recordings of human driving and could not be directly used during simulation since the evaluated E2E-AD methods could behave differently from experts.

During simulation as shown in Fig. 2, at each step, (1)The evaluated **E2E-AD agent yields a planned trajectory**  $\text{Tr}_t = \{(x_i, y_i)\}_{i=1}^{T_f}$  based on current images  $\mathbf{I}_t$  and ego states  $\mathbf{E}_t$ , where  $T_f$  is the length of prediction. (2) Then, the **behavioral controller executes the predicted trajectory  $\text{Tr}_t$  and generates behaviors** of other driving agents to update bounding boxes, map elements, and ego status. In this work, we adopt nuPlan’s rule-based IDM policy [83] while it could also be learning-based models [51] for traffic simulation [46]. (3) Finally, the proposed **generative renderer generates new surrounding images  $\mathbf{I}_{t+1}$**  based on aforementioned information in the scene. The three steps are iteratively executed during the closed-loop simulation.

### 3.3. Generative Renderer

The key innovation of Bench2Drive-R is the generative renderer, which is composed of Latent Diffusion Model (we adopt pretrained Stable Diffusion v1.5) and ControlNet. As shown in Fig. 3, we unify multiple simulation oriented designs into a ControlNet encoder to achieve controllable, consistent, and interactive surrounding image generation in AD scenarios based on given conditions from behavioral controller and database. We demonstrate the details in the following sections.

#### 3.3.1 Temporal Consistency Module & Mitigation of Autoregressive Distribution Shift

Different from video diffusion models [2, 3, 28] which improve temporal consistency by introducing attention along temporal axis of the noise, Bench2Drive-R, as an autoregressive interactive generation method, improves temporal consistency by encoding previously generated images  $\mathbf{I}_{t-1}$  with ControlNet [108]. Specifically, We encode  $\mathbf{I}_{t-1}$  into latent space with the same VAE encoder as Stable Diffusion’s and send it into the ControlNet encoder. The output hidden features from each layer of ControlNet are directly added to the corresponding layers of the U-Net encoder, as in Fig. 3.

However, utilizing the previous image introduces a train-val gap issue. During training, the previous images are always ground-truth while during inference, previous images are from generation which have gaps with real world ones, even slightly. As a result, due to the recurrent nature of autoregressive generation, the error accumulates and could finally collapse the generation, as shown in Fig.4 (Left). It is called teacher-forcing [49] or distribution shift [74] issue.

Since the deterioration stems from over-reliance on pre-

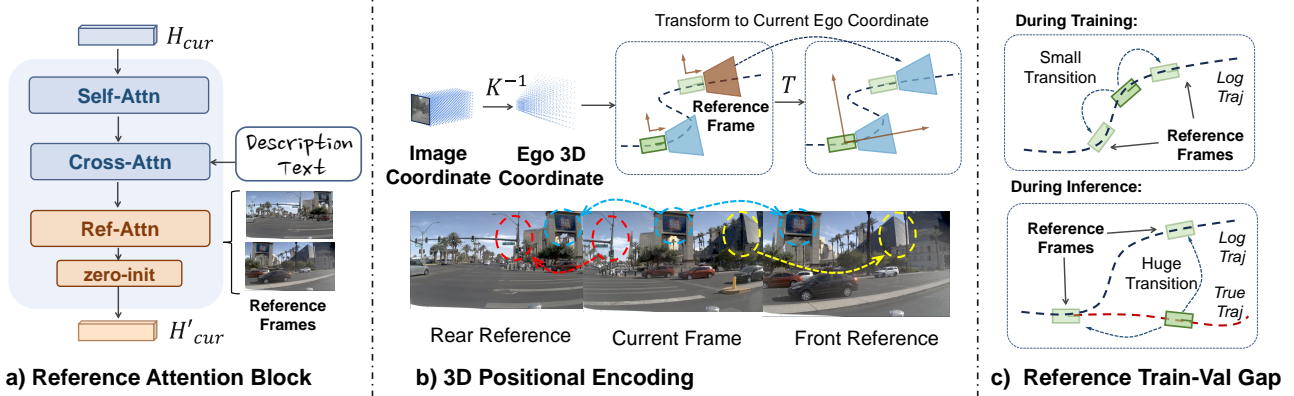


Figure 5. **Designs for Retrieval based Scene-Level Control.** a) Reference images are utilized in ControlNet with an additional cross attention module (Ref-Attn). b) Pixel-level 3D position encodings are calculated and fed into cross attention to provide spatial relations between reference and current images. c) E2E-AD agents might not follow logged trajectory during inference, leading to train-val gap.

vious images [84], we propose **noise modulation with Gaussian blur** to address the issue. Specifically, during training, previous-frame images are firstly encoded into latent space to get conditional previous latent  $z_{\text{prev}}$ . Then a random level of Gaussian noise is added to  $z_{\text{prev}}$ . The noise level is also input into the ControlNet encoder, which can be formulated as:

$$c_{\text{prev}} = \mathcal{E}(\sqrt{\bar{\alpha}_n} z_{\text{prev}} + \sqrt{1 - \bar{\alpha}_n} \epsilon; n) \quad (2)$$

where  $\mathcal{E}$  represents the ControlNet encoder;  $\epsilon \in \mathcal{N}(0, 1)$  is the randomly sampled Gaussian noise and  $n \in \mathcal{U}[0, N]$ . The noise-adding policy is similar to the training strategy of diffusion models [27, 77], where the noise level  $n$  here is analogous to the timestep  $t$  in diffusion models. To further avoid accumulation of high-frequency artifacts, we apply Gaussian blurring to previous-frame images. As shown in Fig. 4 and later experiments, the proposed techniques could effectively alleviate the deterioration issue.

### 3.3.2 Projected Object-Level Control

This module follows existing generative models for AD [87, 89] and *we do not claim it as our contributions*. During simulation, the object-level information  $\mathbf{B}_t$  and  $\mathbf{M}_t$  is available from behavioral controller. Thus, to adopt them as control information, we project 3D bounding boxes  $\mathbf{B}_t$  and vectorized map elements  $\mathbf{M}_t$  Lidar coordinate system to 2D perspective view using the provided camera parameters  $\mathbf{P}$  [20, 87, 89]. Then we plot the projected discrete coordinates to form a set of binary masks of the same size with input images  $\mathbf{B}_t^{\text{mask}} \in \mathbb{R}^{|\mathcal{C}_{\text{box}}| \times H \times W}$  and  $\mathbf{M}_t^{\text{mask}} \in \mathbb{R}^{|\mathcal{C}_{\text{map}}| \times H \times W}$ . We incorporate object semantic information by assigning each class its own dedicated channel. The two kinds of object level controls are concatenated and encoded into the latent space with a simple convolutional network.

Then, these encoded control signals are injected into the denoising process using the same ControlNet encoder described in Section 3.3.1. Our projected object-level control can be formulated as:

$$c_{\text{proj}} = \mathcal{E}(\text{Conv}(\text{Cat}(\mathbf{B}_t^{\text{mask}}, \mathbf{M}_t^{\text{mask}}))) \quad (3)$$

### 3.3.3 Retrieval based Scene-Level Control

Generative models are susceptible to creating fictitious artifacts [16]. Previous studies on generative models for autonomous driving have primarily focused on generating a diverse range of driving scenes [20, 89] to enhance the ground-truth dataset, effectively serving as a form of data augmentation. By contrast, **for the proposed simulation framework, fidelity is the most important factor for generative renderer since the tasks of enhancing diversity is assigned to the initial scenario selection and the behavioral controller**. In other words, we expect the diffusion models to faithfully follow controls and conditions, akin to a meticulous oil painter, rather than behaving like an artist who seeks to create diverse interpretations.

To achieve this, **one key observation is that the background of scene could be deterministically decided by referring to recordings  $\{(\text{coord}_i, \mathbf{I}_i)\}_{i=1}^{N_f}$  since the background is static**. Thus, for high fidelity, extra control conditions could be applied by retrieval to eliminate uncertainty. Specifically, **the two frames within recordings with closest distance** (one from ahead of the ego vehicle and one from behind) to current location of ego agent are retrieved:

$$\mathcal{P} = \{(\text{coord}_i - \text{coord}_{\text{ego}}) \cdot \mathbf{v}_{\text{ego}}\}_{i=1}^{N_f} \quad (4)$$

$$\mathbf{I}_{\text{ref}}^{\text{front}} = \mathbf{I} \left[ \underset{i; \mathcal{P}_i > 0}{\text{argmin}} \mathcal{P}_i \right]; \quad \mathbf{I}_{\text{ref}}^{\text{rear}} = \mathbf{I} \left[ \underset{i; \mathcal{P}_i < 0}{\text{argmax}} \mathcal{P}_i \right]$$

The two retrieved images are encoded by an image encoder (e.g., ResNet) and put into ControlNet as key and value in



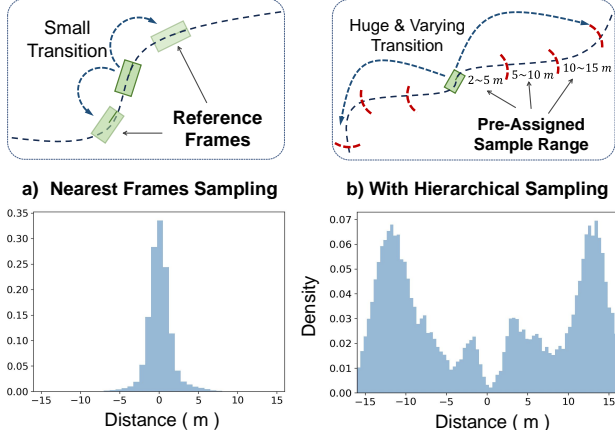


Figure 6. **Different Sampling Strategies for Reference Frames during Training.** a) Simply retrieving the closest one would make the model only be able to deal with very similar reference images. b) The proposed hierarchical sampling strategy forces the model adapts to reference images from a large scale of distance range.

an additional cross-attention module so that the generation of current frames could find correspondence of background.

Further, since the spatial relations between current frame and the two reference frames could be explicitly calculated based on coordinate transformation, **we consider injecting pixel-wise spatial relations information into cross attention.** Specifically, pixel-wise 3D position encodings are adopted similarly to [59, 60]. A discrete meshgrid  $\mathbf{P}$  of size  $(H, W, D, 4)$  in camera frustum space is calculated for all images, where  $D$  is the number of points sampled along the depth axis. Then, the meshgrid is transformed from camera frustum space to current ego coordinate system with camera transformation matrix  $\mathbf{P}^{\text{lidar}} = \mathbf{K}^{-1}\mathbf{P}$  for both current frame  $\mathbf{P}_{\text{ego}}$  and the two reference frames  $\mathbf{P}_{\text{ref}}$ . Finally,  $\mathbf{P}_{\text{ego}}$  serves as the PE of query while  $\mathbf{P}_{\text{ref}}$  serves as PE of key within the cross attention of ControlNet (Fig. 5 (a)(b)):

$$H'_{\text{cur}} = \text{Attn}(Q = H_{\text{cur}} + \mathbf{P}_{\text{ego}}, K = H_{\text{ref}} + \mathbf{P}_{\text{ref}}, V = H_{\text{ref}}) \quad (5)$$

which enables the current frame to find the correspondence in reference images so that it can follow the static background and generate the transformed pixels.

By utilizing retrieval-based conditions, the street scene on both sides of the ego vehicle is deterministic and the generative renderer is only responsible for generating coherent images. However, this introduces another train-val gap challenge. **During training, if we simply retrieve the nearest images, they would always be the preceding and following frames within a small distance range while during inference, E2E-AD agents could behave differently from experts and thus the distance to reference images could be far,** shown in Fig. 5 (c). As a result, the training would cause the model to overly rely on references and collapse in the large deviation situations during inference.

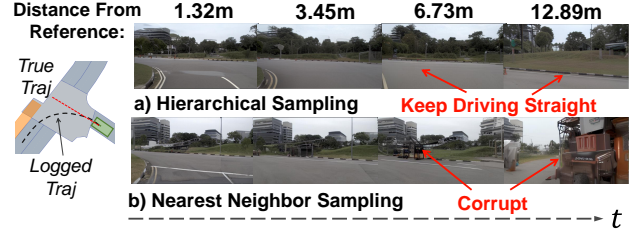


Figure 7. **Case Study on Influence of Different Training Sampling Strategies.** Hierarchical sampling strategy preserves generation quality even under large deviation during inference.

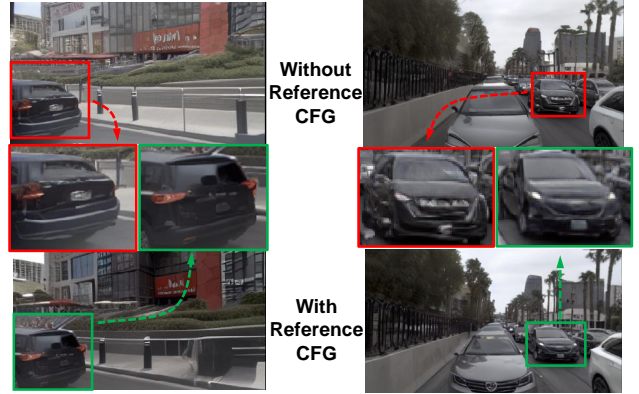


Figure 8. **Reference CFG** lessens reliance on reference frames and enhances foreground object authenticity.

To address the issue, we propose to **let the model see reference images in a wide range of distance during training.** Specifically, for each training sample, we employ a hierarchical sampling technique where reference images are selected out of one of the three distance intervals (2m-5m, 5m-10m, or 10m-15m) based on a pre-assigned probability to balance the sampling. In this work, we assign the probability to be (0.1, 0.3, 0.6), significantly increasing long-distance samples compared with simple nearest frames sampling, as in Fig. 6. The proposed sampling makes the model adapt to highly divergent reference images, effectively narrowing the train-val gap and notably improving the generation quality and model’s numerical stability. Fig. 7 gives an example of long-range deviation and the generation results under different training strategies.

Further, we observe that the generation process might overly rely on reference images and thus leads to bad generalization ability. To alleviate the issue, we apply classifier-free guidance (CFG) [26] to reference image, dubbed reference CFG, where we randomly substitute reference images with empty images during training. Similar to standard CFG, at each denoising step during inference, we weighted sum the two predicted noise, one with reference images and one without. As shown in Fig. 8, reference-CFG alleviates model’s reliance on reference image, resulting in more au-

Table 2. Comparisons of FID, 3D object detection and BEV segmentation on nuScenes validation set. \* means our replication.

Method	FID	BEVFormer [55]			BEVFusion [61] (Camera Branch)				StreamPETR [86]	
		NDS↑	mAP↑	mAOE↓	NDS↑	mAP↑	mAOE↓	mIoU ↑	NDS↑	mAP↑
Oracle	-	53.50	45.61	0.35	41.20	35.53	0.56	57.09	57.10	48.20
BEVControl [99]	24.85	28.68	19.64	0.78	-	-	-	-	-	-
MagicDrive* [20]	16.20	25.76	14.07	0.79	23.35	12.54	0.77	28.94	35.51	21.41
Panacea [89]	16.69	-	-	-	-	-	-	-	32.10	-
Panacea+ [90]	15.50	-	-	-	-	-	-	-	34.60	-
Bench2Drive-R	<b>10.95</b>	<b>34.70</b>	<b>20.11</b>	<b>0.48</b>	<b>25.75</b>	<b>13.53</b>	<b>0.73</b>	<b>42.75</b>	<b>40.23</b>	<b>24.04</b>

Table 3. Performance of UniAD’s Different Tasks in nuScenes. \* means our replication.

Method	Detection		BEV Segmentation				Planning		Occupancy
	NDS [4]↑	mAP↑	Lanes↑	Drivable↑	Divider↑	Crossing↑	avg.L2(m)↓	avg.Col.↓	mIoU↑
Oracle	49.85	37.98	31.31	69.14	25.93	14.36	1.05	0.29	63.7
MagicDrive* [20]	29.35	14.09	23.73	55.28	18.83	6.57	1.18	0.33	54.6
Bench2Drive-R	<b>33.04</b>	<b>15.16</b>	<b>25.5</b>	<b>56.53</b>	<b>21.27</b>	<b>8.67</b>	<b>1.15</b>	<b>0.31</b>	<b>55.5</b>

thetic foreground objects generation.

## 4. Experiment

### 4.1. Experimental Setups

#### 4.1.1 Dataset

We conduct detection evaluation and open-loop planning evaluation on **nuScenes dataset** [4] and closed-loop planning evaluation on **nuPlan dataset** [46].

We use the nuScenes’s official train-val-test split while for nuplan, we use the mini split (around 5 times larger than nuScenes) due to limited computational resource.

#### 4.1.2 Training and Inference

We base the behavior controller in our framework on nuPlan [46] simulators and our generative renderer on SDv1.5 [72]. Pretrained weights are used to initialize the U-Net layers.

At the training stage, we optimize our renderer for 50k steps with a total batch-size of 114 on nuScenes, and for 140k steps with a total batch-size of 64 on nuPlan. The learning rate is set to be  $1e-4$  and cosine-annealing scheduler is employed with warm-up steps to be 3k steps. We assign the drop-out rate of retrieved reference images to be 0.2, and Reference CFG’s guidance scale is set to be 2 at inference time.

During inference, following [20], images are sampled using the UniPC [114] scheduler for 20 steps. All sensor images are sampled at a spatial resolution of  $400 \times 224$  and then upsampled to the original size with bicubic [47] interpolation, namely  $1600 \times 900$  for nuScenes and  $2000 \times 1200$  for nuPlan. We use the official UniAD pretrained weight on

nuScenes and train an 8-views version of VAD on nuPlan dataset. Although the simulation frequency of nuPlan simulator is 10Hz, we follow the convention in the community and set the inference frequency of VAD to be 2Hz, and use the most recently predicted trajectory to propagate world state at the intermediate frames.

#### 4.1.3 Metrics

Following existing works, we evaluate the **generation quality** with Frechet Inception Distance (FID) [25], which measures the distance between the distributions of real and generated images, reflecting image synthesis quality. The **layout conformity** of Bench2Drive-R generative renderer is evaluated through performing object detection and BEV segmentation on the generated images. Widely used baselines BEVFormer [55] and BEVFusion [61] (camera branch) are selected. To evaluate the **temporal consistency** of the generated image sequence, we employ state-of-the-art streaming perception models StreamPETR [86]. StreamPETR features the reuse of agent queries from previous frames and thus improved perception scores indicate better temporal consistency. To evaluate the influence on **planning**, we employ UniAD [32] and VAD [45] for open-loop and closed-loop evaluation respectively.

For closed-loop evaluation, we employ **CLS** (Closed-Loop Score) defined by the official nuPlan challenge. CLS is a scenario-based metric, which comprehensively combine multiple aspects of driving performance assessments including drivable area compliance, collision time, progress along the driving direction, comfort, etc.

Table 4. Open-Loop Planning Ablation

Temporal Consistency	Retrieval Ref	FID	Detection NDS $\uparrow$	Planning avg.L2(m) $\downarrow$
$\times$	$\times$	21.06	21.80	1.19
$\checkmark$	$\times$	14.04	25.75	1.17
$\checkmark$	$\checkmark$	<b>10.95</b>	<b>33.04</b>	<b>1.15</b>

Table 5. Noise &amp; Gaussian Blur Ablation

Noise Modulation	Gaussian Blur	FID			
		0.5s	1s	1.5s	2s
$\times$	$\times$	<b>12.68</b>	16.09	23.77	31.79
$\checkmark$	$\times$	14.87	17.64	18.72	19.58
$\checkmark$	std=1	14.40	<b>16.84</b>	<b>18.01</b>	<b>18.67</b>
$\checkmark$	std=2	15.55	18.14	19.11	19.79

Table 6. Closed-Loop Planning

Methods	BEVFormer		R-CLS
	NDS $\uparrow$	mAP $\uparrow$	
Log-Replay	0.05	0.03	27.24
No Ref & No Prev	23.31	12.21	28.56
Bench2Drive-R	<b>28.23</b>	<b>17.23</b>	<b>30.49</b>

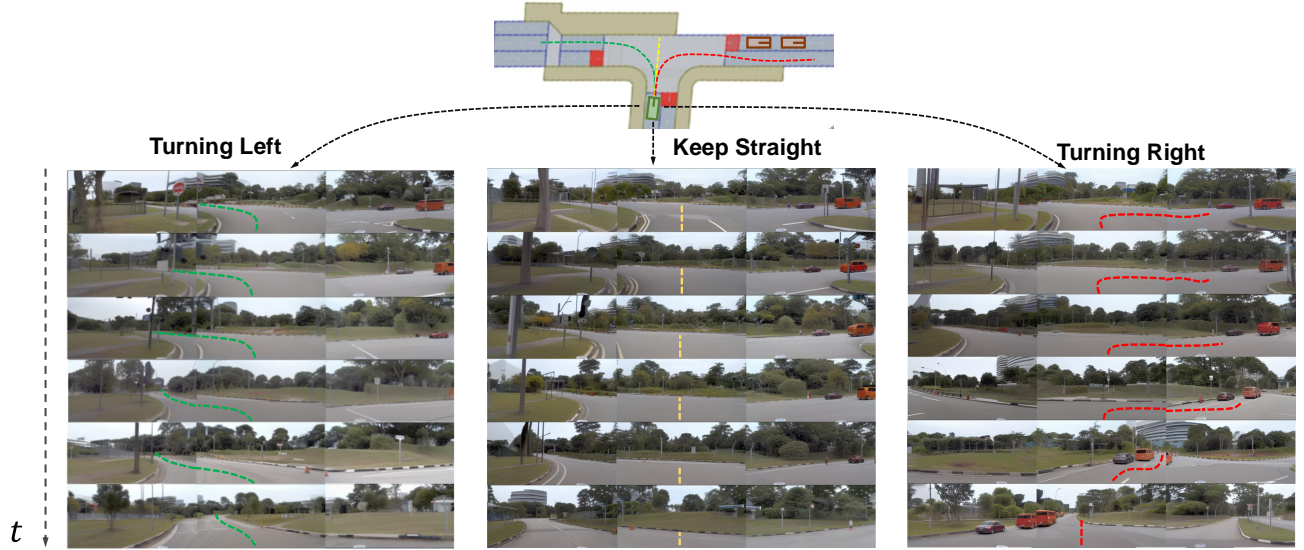


Figure 9. Closed-Loop Interactive Simulation in nuPlan. Generated image sequences under three different E2E-AD agent behaviors.

## 4.2. Main Results

### 4.2.1 Quantitative Analysis

**Generation Quality and Controllability.** We evaluate the generation capability of Bench2Drive-R’s generative renderer with nuScenes validation dataset. As shown in Tab. 2, Bench2Drive-R outperforms baselines BEVControl [99], MagicDrive [20], Panacea [89] and Panacea+ [90] in generation quality, yielding notably lower FID score. For controllability, better perception and segmentation scores are achieved on Bench2Drive-R-generated images, indicating better generation precision for objects and map elements.

**Temporal Consistency.** Bench2Drive-R can yield consistent sensor image sequence over a long horizon, which is crucial for perception models with high temporal reliance. As shown in Tab. 2, perception scores with StreamPETR are notably better than the baseline method. This demonstrates the effectiveness of our method in improving temporal consistency under autoregressive generation setting.

**Open-Loop Evaluation.** As in Tab. 3, UniAD performs better on Bench2Drive-R generated image sequences than baselines under nuScenes open-loop evaluation protocol.

**Closed-Loop Planning.** We integrate the Bench2Drive-R framework into nuPlan for **closed-loop reactive simula-**

**tion.** We adopt the Val14 evaluation split [14]. However, since only 10% scenes in nuPlan have sensor data, we filter 10 full clips from each of the 14 scenarios and report R-CLS score and perception score. We use two simple image acquisition methods to serve as baselines, log replaying (collecting images with corresponding timestep from recorded ego trajectories) and static frame generation with no previous prior or reference frames.

As is shown in Tab. 6, Bench2Drive-R’s perception scores are notably higher than baseline methods, indicating sensor images’ great adherence to bbox-level simulation environment and the efficacy of our methods. However, R-CLS of VAD exhibits only a marginal improvement. This is because VAD, which adopts an imitation learning paradigm, is not capable of coping with long horizon closed-loop simulation, which is aligned with previous findings [9]. Driving scores of VAD tend to drop to zero at the early stage of simulations due to its limited capability. We provide more case studies for VAD planning ability in Section 4.4.

### 4.2.2 Qualitative Analysis

**Closed-Loop Interactive Simulation.** As in Fig. 9, Bench2Drive-R is able to generate high-fidelity images under different behaviors of E2E-AD agents.



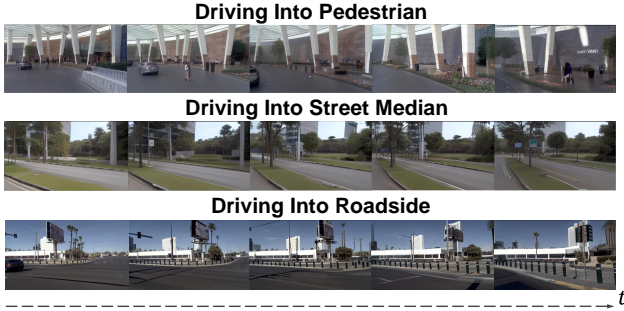


Figure 10. **Generalizability.** Out-of-distribution generation results under scenarios absent in the training dataset.

**Generalizability.** As in Fig. 10, Bench2Drive-R can generate authentic sensor images even under scenarios absent in training dataset, demonstrating the rich real-world prior knowledge in the pretrained diffusion model.

### 4.3. Ablative Study

**Designs of Generative Renderer.** In Tab. 4, we ablate the two proposed simulation oriented designs and results show that task performance improves along with the modules we add, demonstrating their effectiveness.

**Noise Modulation with Gaussian Blurring** As shown in Tab. 5, directly encoding previous images leads to fast deterioration while with noise modulation and a proper level of Gaussian noise added, generalization quality remains stable during autoregressive generation process.

**3D Positional Encoding.** As shown in Fig. 11, with the explicit spatial transformation information provided by 3D PE, generated images exhibit pixel-level correspondence.

### 4.4. Analysis on VAD Planning Performance

We provide some typical failure cases of VAD in Fig. 12. As suggested by Fig. 12 (a) and (b), VAD is hard to start from static states, and is unable to slow down even when there are slow cars in the front. This proves the findings [9, 105] that imitation based driving models are likely to take shortcuts from current kinetic states during training, developing an overly reliance on ego states while ignoring other information during inference.

In Fig 12 (c), VAD’s planning results are very close to ground-truth trajectory at the early stage of a left turn. However, the ego car gradually deviates from the original route because of accumulated errors and the model can’t adapt to the changes and hit the roadblock. This result intermediately reflects that the now commonly-used open-loop protocols is not capable of evaluating model’s true driving ability.

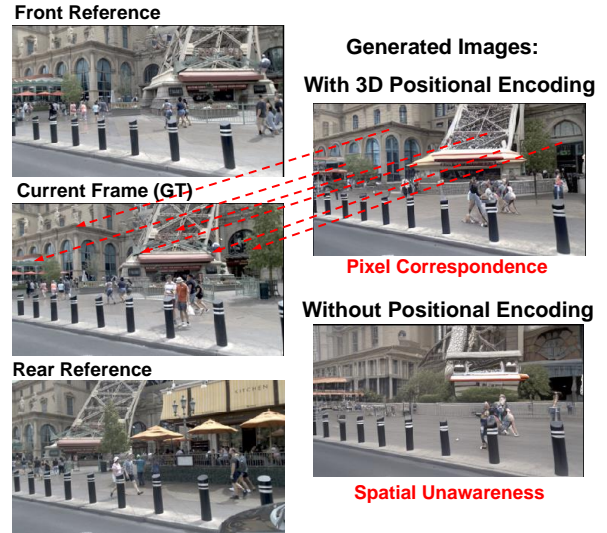


Figure 11. **Effect for 3D Positional Encoding.** 3D PE provides explicit spatial transition information, which effectively avoids spacial unawareness.

## 5. More Qualitative Results

### 5.1. Generation Quality

As shown in Fig. 14, Bench2Drive-R is capable of generating high-fidelity panoramic images under diverse driving scenarios.

### 5.2. Controllability & Spacial Consistency

We demonstrate the controllability of Bench2Drive-R by removing all object bounding boxes in a driving scenarios, as shown in Fig. 13. For each scenario, we generate two sets of images, one with bounding boxes and one without. Despite the radical changes of object control signals, Bench2Drive-R is able to achieve high spacial consistency at the background level and removes all foreground objects in the scenario (including driving cars and pedestrians), demonstrating the efficacy of our designs for the generative renderer.

### 5.3. More Interactive Simulation Visualization

We provide more interactive simulation results in Fig. 15 16 17. For each driving scenario, we let the ego driving agent conduct two different behaviors. Bench2Drive-R ensures great spatial-temporal consistency, providing a coherent simulation environment.

## 6. Conclusion

We present Bench2Drive-R, a simulation-oriented generative framework that enables reactive closed-loop evaluation for end-to-end driving models. We prove the efficacy of the simulation-oriented designs through thorough experiments.



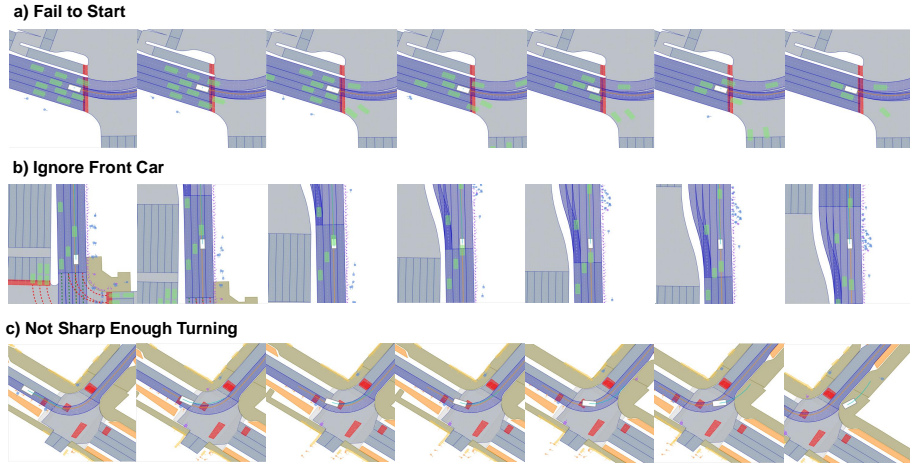


Figure 12. **Typical Failure Cases of VAD** We select three typical failure cases of VAD: failing to start, accelerating when there are cars in the front and failing to take turns. The white box is the ego car; green boxes are other driving cars; the green line is the planned ego trajectory and the orange line is logged expert trajectory.

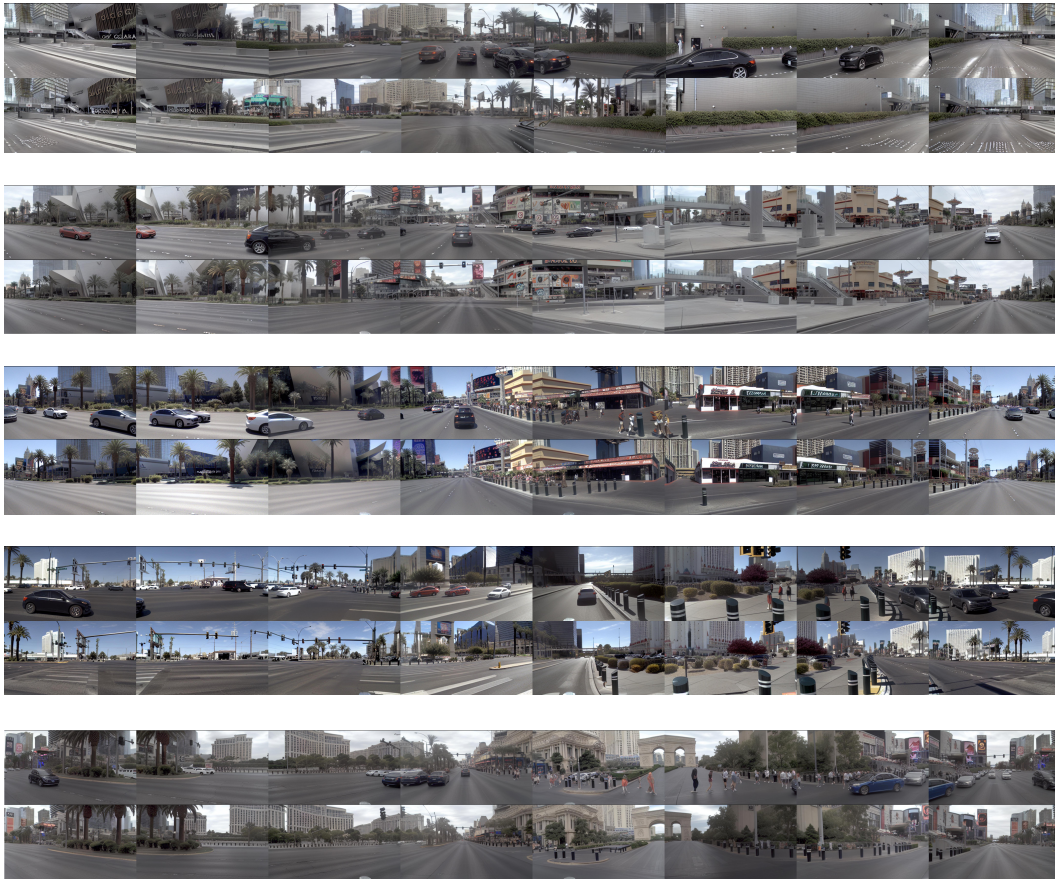


Figure 13. **Controllability and Spatial Consistency** For each set of images, the upper row is generated with object bounding boxes and the lower row without. Bench2Drive-R abides strictly by the control signals while maintaining high background consistency.



nuScenes



nuPlan



Figure 14. **Generated Images In NuScenes and NuPlan.** Bench2Drive-R is capable of generating diverse driving scenarios with high fidelity.



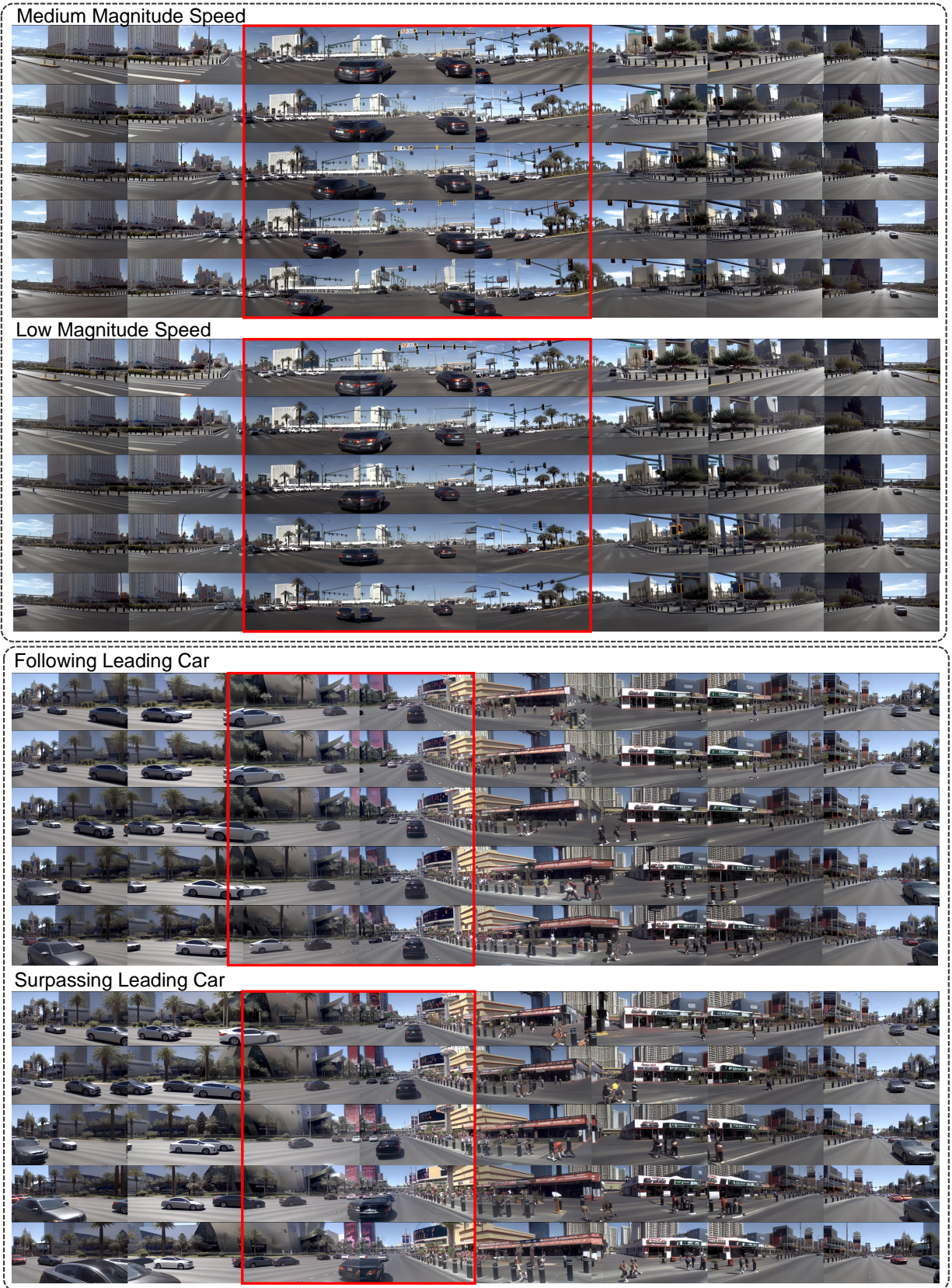


Figure 15. **Interactive Simulation Result.** Views with most conspicuous differences are highlighted with red boxes.



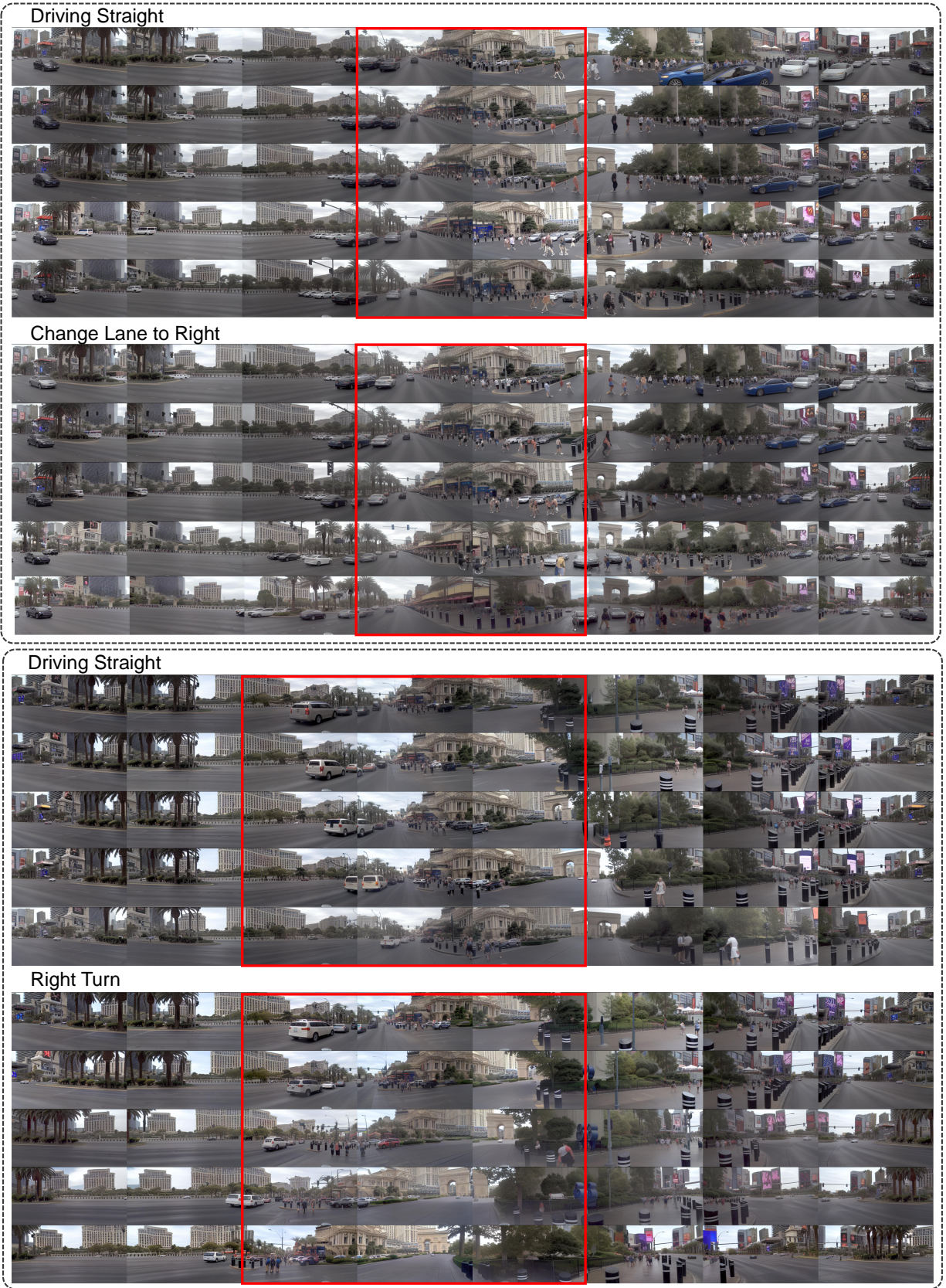


Figure 16. **Interactive Simulation Result.** Views with most conspicuous differences are highlighted with red boxes.



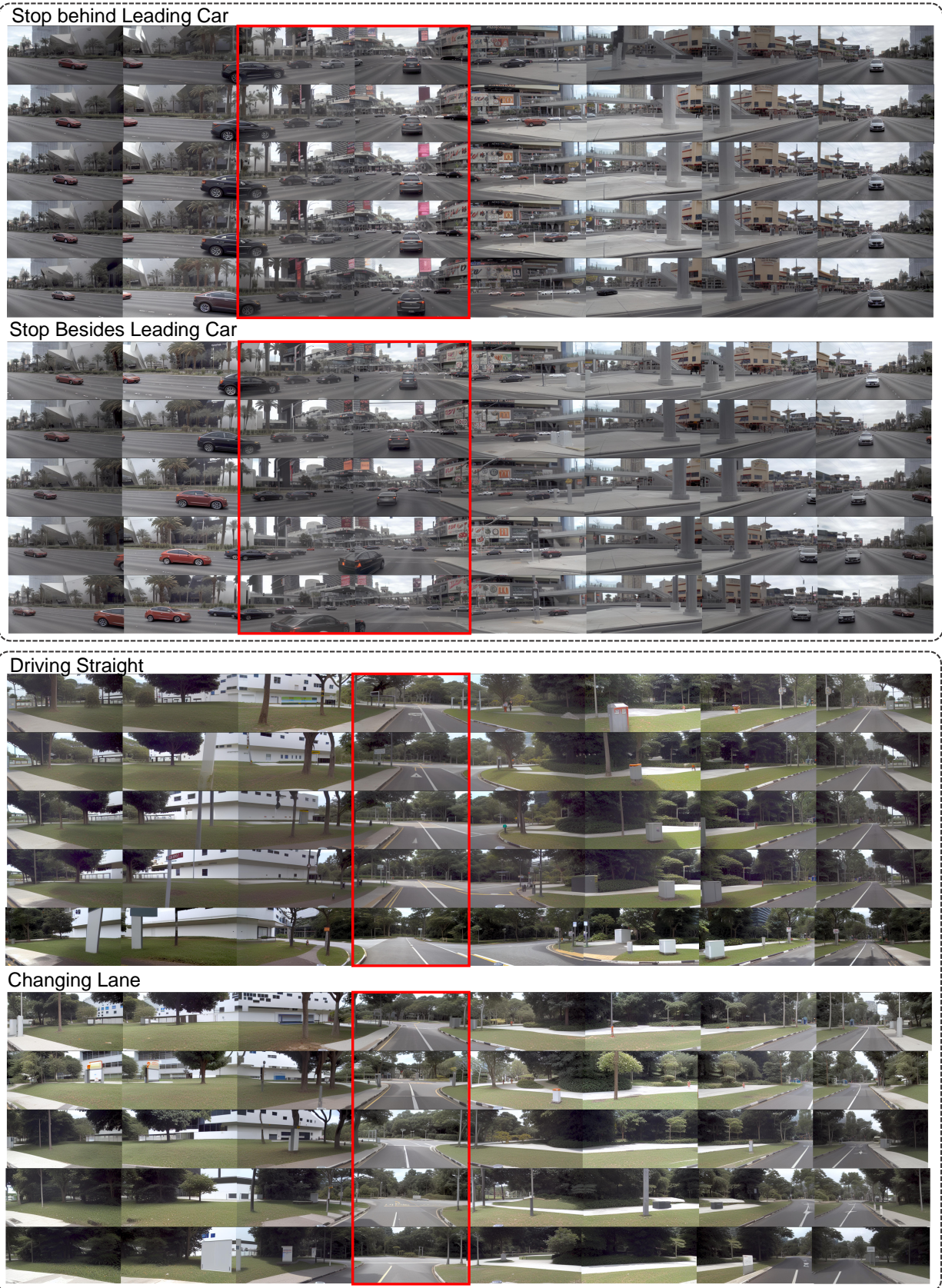


Figure 17. **Interactive Simulation Result.** Views with most conspicuous differences are highlighted with red boxes.

## References

- [1] Akhil Bandarupalli, Adithya Bhat, Saurabh Bagchi, Aniket Kate, Chen-Da Liu-Zhang, and Michael K. Reiter. Delphi: Efficient asynchronous approximate agreement for distributed oracles. *arXiv preprint arXiv:2405.02431*, 2024. 3, 4
- [2] Andreas Blattmann, Tim Dockhorn, Sumith Kulal, Daniel Mendeleevitch, Maciej Kilian, Dominik Lorenz, Yam Levi, Zion English, Vikram Voleti, Adam Letts, Varun Jampani, and Robin Rombach. Stable video diffusion: Scaling latent video diffusion models to large datasets. *arXiv preprint arXiv:2311.15127*, 2023. 5
- [3] Andreas Blattmann, Robin Rombach, Huan Ling, Tim Dockhorn, Seung Wook Kim, Sanja Fidler, and Karsten Kreis. Align your latents: High-resolution video synthesis with latent diffusion models. *arXiv preprint arXiv:2304.08818*, 2023. 5
- [4] Holger Caesar, Varun Bankiti, Alex H. Lang, Sourabh Vora, Venice Erin Liong, Qiang Xu, Anush Krishnan, Yu Pan, Giancarlo Baldan, and Oscar Beijbom. nuscenes: A multi-modal dataset for autonomous driving. In *CVPR*, 2020. 1, 3, 8
- [5] Dian Chen and Philipp Krähenbühl. Learning from all vehicles. In *CVPR*, 2022. 3
- [6] Dian Chen, Brady Zhou, Vladlen Koltun, and Philipp Krähenbühl. Learning by cheating. In *CoRL*, pages 66–75. PMLR, 2020. 3
- [7] Yurui Chen, Chun Gu, Junzhe Jiang, Xiatian Zhu, and Li Zhang. Periodic vibration gaussian: Dynamic urban scene reconstruction and real-time rendering. *arXiv preprint arXiv:2311.18561*, 2024. 4
- [8] Ziyu Chen, Jiawei Yang, Jiahui Huang, Riccardo de Lutio, Janick Martinez Esturo, Boris Ivanovic, Or Litany, Zan Gojic, Sanja Fidler, Marco Pavone, Li Song, and Yue Wang. Omnire: Omni urban scene reconstruction. *arXiv preprint arXiv:2408.16760*, 2024. 4
- [9] Jie Cheng, Yingbing Chen, Xiaodong Mei, Bowen Yang, Bo Li, and Ming Liu. Rethinking imitation-based planner for autonomous driving. *arXiv preprint arXiv:2309.10443*, 2023. 9, 10
- [10] Kashyap Chitta, Aditya Prakash, Bernhard Jaeger, Zehao Yu, Katrin Renz, and Andreas Geiger. Transfuser: imitation with transformer-based sensor fusion for autonomous driving. *TPAMI*, 2022. 3
- [11] Kashyap Chitta, Aditya Prakash, Bernhard Jaeger, Zehao Yu, Katrin Renz, and Andreas Geiger. Transfuser: Imitation with transformer-based sensor fusion for autonomous driving. *Pattern Analysis and Machine Intelligence (PAMI)*, 2023. 1
- [12] Felipe Codevilla, Matthias Müller, Antonio López, Vladlen Koltun, and Alexey Dosovitskiy. End-to-end driving via conditional imitation learning. In *ICRA*, pages 4693–4700, 2018. 3
- [13] Felipe Codevilla, Eder Santana, Antonio M López, and Adrien Gaidon. Exploring the limitations of behavior cloning for autonomous driving. In *CVPR*, pages 9329–9338, 2019. 3
- [14] Daniel Dauner, Marcel Hallgarten, Andreas Geiger, and Kashyap Chitta. Parting with misconceptions about learning-based vehicle motion planning. *arXiv preprint arXiv:2306.07962*, 2023. 1, 3, 9
- [15] Daniel Dauner, Marcel Hallgarten, Tianyu Li, Xinshuo Weng, Zhiyu Huang, Zetong Yang, Hongyang Li, Igor Gilitschenski, Boris Ivanovic, Marco Pavone, Andreas Geiger, and Kashyap Chitta. Navsim: Data-driven non-reactive autonomous vehicle simulation and benchmarking. *arXiv preprint arXiv:2406.15349*, 2024. 1, 3
- [16] Decart, Julian Quevedo, Quinn McIntyre Spruce Campbell, Xinlei Chen, and Robert Wachen. Oasis: A universe in a transformer. 2024. 6
- [17] Boyang Deng, Richard Tucker, Zhengqi Li, Leonidas Guibas, Noah Snavely, and Gordon Wetzstein. Streetscapes: Large-scale consistent street view generation using autoregressive video diffusion. *arXiv preprint arXiv:2407.13759*, 2024. 4
- [18] Alexey Dosovitskiy, German Ros, Felipe Codevilla, Antonio Lopez, and Vladlen Koltun. Carla: An open urban driving simulator. In *CoRL*, pages 1–16. PMLR, 2017. 1, 3
- [19] Lue Fan, Hao Zhang, Qitai Wang, Hongsheng Li, and Zhaoxiang Zhang. Freesim: Toward free-viewpoint camera simulation in driving scenes. *arXiv preprint arXiv:2412.03566*, 2024. 4
- [20] Ruiyuan Gao, Kai Chen, Enze Xie, Lanqing Hong, Zhen-guo Li, Dit-Yan Yeung, and Qiang Xu. Magicdrive: Street view generation with diverse 3d geometry control. *arXiv preprint arXiv:2310.02601*, 2024. 2, 4, 6, 8, 9
- [21] Shenyuan Gao, Jiazhi Yang, Li Chen, Kashyap Chitta, Yihang Qiu, Andreas Geiger, Jun Zhang, and Hongyang Li. Vista: A generalizable driving world model with high fidelity and versatile controllability. *arXiv preprint arXiv:2405.17398*, 2024. 2, 3, 4



- [22] Cole Gulino, Justin Fu, Wenjie Luo, George Tucker, Eli Bronstein, Yiren Lu, Jean Harb, Xinlei Pan, Yan Wang, Xiangyu Chen, John D. Co-Reyes, Rishabh Agarwal, Rebecca Roelofs, Yao Lu, Nico Montali, Paul Mouglin, Zoey Yang, Brandyn White, Aleksandra Faust, Rowan McAllister, Dragomir Anguelov, and Benjamin Sapp. Waymax: An accelerated, data-driven simulator for large-scale autonomous driving research. *arXiv preprint arXiv:2310.08710*, 2023. 3
- [23] Jianfei Guo, Nianchen Deng, Xinyang Li, Yeqi Bai, Botian Shi, Chiyu Wang, Chenjing Ding, Dongliang Wang, and Yikang Li. Streetsurf: Extending multi-view implicit surface reconstruction to street views. *arXiv preprint arXiv:2306.04988*, 2023. 4
- [24] Xi Guo, Chenjing Ding, Haoxuan Dou, Xin Zhang, Weixuan Tang, and Wei Wu. Infinitydrive: Breaking time limits in driving world models. *arXiv preprint arXiv:2412.01522*, 2024. 4
- [25] Martin Heusel, Hubert Ramsauer, Thomas Unterthiner, Bernhard Nessler, and Sepp Hochreiter. Gans trained by a two time-scale update rule converge to a local nash equilibrium. *Advances in neural information processing systems*, 30, 2017. 8
- [26] Jonathan Ho and Tim Salimans. Classifier-free diffusion guidance. *arXiv preprint arXiv:2207.12598*, 2022. 7
- [27] Jonathan Ho, Ajay Jain, and Pieter Abbeel. Denoising diffusion probabilistic models. *arXiv preprint arXiv:2006.11239*, 2020. 2, 3, 6
- [28] Jonathan Ho, Tim Salimans, Alexey Gritsenko, William Chan, Mohammad Norouzi, and David J. Fleet. Video diffusion models. *arXiv preprint arXiv:2204.03458*, 2022. 5
- [29] Anthony Hu, Gianluca Corrado, Nicolas Griffiths, Zak Murez, Corina Gurau, Hudson Yeo, Alex Kendall, Roberto Cipolla, and Jamie Shotton. Model-based imitation learning for urban driving. *NeurIPS*, 2022. 3
- [30] Anthony Hu, Lloyd Russell, Hudson Yeo, Zak Murez, George Fedoseev, Alex Kendall, Jamie Shotton, and Gianluca Corrado. Gaia-1: A generative world model for autonomous driving. *arXiv preprint arXiv:2309.17080*, 2023. 2, 3, 4
- [31] Shengchao Hu, Li Chen, Penghao Wu, Hongyang Li, Junchi Yan, and Dacheng Tao. St-p3: End-to-end vision-based autonomous driving via spatial-temporal feature learning. In *ECCV*, 2022. 3
- [32] Yihan Hu, Jiazhi Yang, Li Chen, Keyu Li, Chonghao Sima, Xizhou Zhu, Siqi Chai, Senyao Du, Tianwei Lin, Wenhai Wang, et al. Planning-oriented autonomous driving. In *CVPR*, pages 17853–17862, 2023. 1, 3, 8
- [33] Binyuan Huang, Yuqing Wen, Yucheng Zhao, Yaosi Hu, Yingfei Liu, Fan Jia, Weixin Mao, Tiancai Wang, Chi Zhang, Chang Wen Chen, Zhenzhong Chen, and Xiangyu Zhang. Subjectdrive: Scaling generative data in autonomous driving via subject control. *arXiv preprint arXiv:2403.19438*, 2024. 3, 4
- [34] Nan Huang, Xiaobao Wei, Wenzhao Zheng, Pengju An, Ming Lu, Wei Zhan, Masayoshi Tomizuka, Kurt Keutzer, and Shanghang Zhang. S<sup>3</sup>gaussian: Self-supervised street gaussians for autonomous driving. *arXiv preprint arXiv:2405.20323*, 2024. 4
- [35] Muhammad Zubair Irshad, Sergey Zakharov, Katherine Liu, Vitor Guizilini, Thomas Kollar, Adrien Gaidon, Zsolt Kira, and Rares Ambrus. Neo 360: Neural fields for sparse view synthesis of outdoor scenes. *arXiv preprint arXiv:2308.12967*, 2023. 4
- [36] Bernhard Jaeger, Kashyap Chitta, and Andreas Geiger. Hidden biases of end-to-end driving models. In *ICCV*, 2023. 3
- [37] Fan Jia, Weixin Mao, Yingfei Liu, Yucheng Zhao, Yuqing Wen, Chi Zhang, Xiangyu Zhang, and Tiancai Wang. Adriver-i: A general world model for autonomous driving. *arXiv preprint arXiv:2311.13549*, 2023. 3, 4
- [38] Xiaosong Jia, Liting Sun, Masayoshi Tomizuka, and Wei Zhan. Ide-net: Interactive driving event and pattern extraction from human data. *IEEE Robotics and Automation Letters*, 6(2):3065–3072, 2021. 2
- [39] Xiaosong Jia, Liting Sun, Hang Zhao, Masayoshi Tomizuka, and Wei Zhan. Multi-agent trajectory prediction by combining egocentric and allocentric views. In *Conference on Robot Learning*, pages 1434–1443. PMLR, 2022. 4
- [40] Xiaosong Jia, Li Chen, Penghao Wu, Jia Zeng, Junchi Yan, Hongyang Li, and Yu Qiao. Towards capturing the temporal dynamics for trajectory prediction: a coarse-to-fine approach. In *CoRL*, pages 910–920. PMLR, 2023. 4
- [41] Xiaosong Jia, Penghao Wu, Li Chen, Yu Liu, Hongyang Li, and Junchi Yan. Hdgt: Heterogeneous driving graph transformer for multi-agent trajectory prediction via scene encoding. *IEEE Transactions on Pattern Analysis and Machine Intelligence*, 45(11):13860–13875, 2023. 2
- [42] Xiaosong Jia, Penghao Wu, Li Chen, Jiangwei Xie, Conghui He, Junchi Yan, and Hongyang Li. Think twice before driving: Towards scalable decoders for end-to-end autonomous driving. In *CVPR*, 2023. 3
- [43] Xiaosong Jia, Shaoshuai Shi, Zijun Chen, Li Jiang, Wenlong Liao, Tao He, and Junchi Yan. Amp: Autoregressive motion prediction revisited with next token prediction for autonomous driving. *arXiv preprint arXiv:2403.13331*, 2024. 4
- [44] Xiaosong Jia, Zhenjie Yang, Qifeng Li, Zhiyuan Zhang, and Junchi Yan. Bench2drive: Towards multi-ability benchmarking of closed-loop end-to-end autonomous driving. In *NeurIPS 2024 Datasets and Benchmarks Track*, 2024. 1
- [45] Bo Jiang, Shaoyu Chen, Qing Xu, Bencheng Liao, Jiajie Chen, Helong Zhou, Qian Zhang, Wenyu Liu, Chang Huang, and Xinggang Wang. Vad: Vectorized scene representation for efficient autonomous driving. *ICCV*, 2023. 1, 3, 8
- [46] Napat Karnchanachari, Dimitris Geromichalos, Kok Seang Tan, Nanxiang Li, Christopher Eriksen, Shakiba Yaghoubi, Noushin Mehdipour, Gianmarco Bernasconi, Whye Kit Fong, Yiluan Guo, and Holger Caesar. Towards learning-based planning: the nuPlan benchmark for real-world autonomous driving. *arXiv preprint arXiv:2403.04133*, 2024. 2, 3, 4, 5, 8

- [47] R. Keys. Cubic convolution interpolation for digital image processing. *IEEE Transactions on Acoustics, Speech, and Signal Processing*, 29(6):1153–1160, 1981. 8
- [48] Seung Wook Kim, Jonah Philion, Antonio Torralba, and Sanja Fidler. Drivegan: Towards a controllable high-quality neural simulation. *arXiv preprint arXiv:2104.15060*, 2021. 3, 4
- [49] Alex M Lamb, Anirudh Goyal ALIAS PARTH GOYAL, Ying Zhang, Saizheng Zhang, Aaron C Courville, and Yoshua Bengio. Professor forcing: A new algorithm for training recurrent networks. *Advances in neural information processing systems*, 29, 2016. 5
- [50] Hongyang Li, Chonghao Sima, Jifeng Dai, Wenhai Wang, Lewei Lu, Huijie Wang, Jia Zeng, Zhiqi Li, Jiazhi Yang, Hanming Deng, et al. Delving into the devils of bird’s-eye-view perception: A review, evaluation and recipe. *IEEE Transactions on Pattern Analysis and Machine Intelligence*, 2023. 4
- [51] Qifeng Li, Xiaosong Jia, Shaobo Wang, and Junchi Yan. Think2drive: Efficient reinforcement learning by thinking in latent world model for quasi-realistic autonomous driving (in carla-v2). In *ECCV*, 2024. 5
- [52] Xiaofan Li, Yifu Zhang, and Xiaoqing Ye. Drivingdiffusion: Layout-guided multi-view driving scene video generation with latent diffusion model. *arXiv preprint arXiv:2310.07771*, 2023. 3, 4
- [53] Yuheng Li, Haotian Liu, Qingyang Wu, Fangzhou Mu, Jianwei Yang, Jianfeng Gao, Chunyuan Li, and Yong Jae Lee. Gligen: Open-set grounded text-to-image generation. *arXiv preprint arXiv:2301.07093*, 2023. 3
- [54] Yingyan Li, Lue Fan, Jiawei He, Yuqi Wang, Yuntao Chen, Zhaoxiang Zhang, and Tieniu Tan. Enhancing end-to-end autonomous driving with latent world model. *arXiv preprint arXiv:2406.08481*, 2024. 3
- [55] Zhiqi Li, Wenhai Wang, Hongyang Li, Enze Xie, Chonghao Sima, Tong Lu, Qiao Yu, and Jifeng Dai. Bevformer: Learning bird’s-eye-view representation from multi-camera images via spatiotemporal transformers. *arXiv preprint arXiv:2203.17270*, 2022. 8
- [56] Zhenxin Li, Kailin Li, Shihao Wang, Shiyi Lan, Zhiding Yu, Yishen Ji, Zhiqi Li, Ziyue Zhu, Jan Kautz, Zuxuan Wu, Yu-Gang Jiang, and Jose M. Alvarez. Hydra-mdp: End-to-end multimodal planning with multi-target hydra-distillation. *arXiv preprint arXiv:2406.06978*, 2024. 3
- [57] Zhiqi Li, Zhiding Yu, Shiyi Lan, Jiahao Li, Jan Kautz, Tong Lu, and Jose M. Alvarez. Is ego status all you need for open-loop end-to-end autonomous driving? *arXiv preprint arXiv:2312.03031*, 2024. 1, 3
- [58] Yixun Liang, Xin Yang, Jiantao Lin, Haodong Li, Xiaogang Xu, and Yingcong Chen. Luciddreamer: Towards high-fidelity text-to-3d generation via interval score matching. *arXiv preprint arXiv:2311.11284*, 2023. 4
- [59] Yingfei Liu, Tiancai Wang, Xiangyu Zhang, and Jian Sun. Petr: Position embedding transformation for multi-view 3d object detection. *arXiv preprint arXiv:2203.05625*, 2022. 7
- [60] Yingfei Liu, Junjie Yan, Fan Jia, Shuailin Li, Aqi Gao, Tiancai Wang, Xiangyu Zhang, and Jian Sun. Petr2: A unified framework for 3d perception from multi-camera images. *arXiv preprint arXiv:2206.01256*, 2022. 7
- [61] Zhijian Liu, Haotian Tang, Alexander Amini, Xinyu Yang, Huizi Mao, Daniela Rus, and Song Han. Bevfusion: Multi-task multi-sensor fusion with unified bird’s-eye view representation. *arXiv preprint arXiv:2205.13542*, 2024. 8
- [62] Fan Lu, Yan Xu, Guang Chen, Hongsheng Li, Kwan-Yee Lin, and Changjun Jiang. Urban radiance field representation with deformable neural mesh primitives. *arXiv preprint arXiv:2307.10776*, 2023. 4
- [63] Han Lu, Xiaosong Jia, Yichen Xie, Wenlong Liao, Xi-aokang Yang, and Junchi Yan. Activead: Planning-oriented active learning for end-to-end autonomous driving. *arXiv preprint arXiv:2403.02877*, 2024. 4
- [64] Yifan Lu, Xuanchi Ren, Jiawei Yang, Tianchang Shen, Zhangjie Wu, Jun Gao, Yue Wang, Siheng Chen, Mike Chen, Sanja Fidler, and Jiahui Huang. Infinicube: Unbounded and controllable dynamic 3d driving scene generation with world-guided video models. *arXiv preprint arXiv:2412.03934*, 2024. 4
- [65] Enhui Ma, Lijun Zhou, Tao Tang, Zhan Zhang, Dong Han, Junpeng Jiang, Kun Zhan, Peng Jia, Xianpeng Lang, Haiyang Sun, Di Lin, and Kaicheng Yu. Unleashing generalization of end-to-end autonomous driving with controllable long video generation. *arXiv preprint arXiv:2406.01349*, 2024. 2
- [66] Chong Mou, Xintao Wang, Liangbin Xie, Yanze Wu, Jian Zhang, Zhongang Qi, Ying Shan, and Xiaohu Qie. T2i-adapter: Learning adapters to dig out more controllable ability for text-to-image diffusion models. *arXiv preprint arXiv:2302.08453*, 2023. 3
- [67] Chaojun Ni, Guosheng Zhao, Xiaofeng Wang, Zheng Zhu, Wenkang Qin, Guan Huang, Chen Liu, Yuyin Chen, Yida Wang, Xueyang Zhang, Yifei Zhan, Kun Zhan, Peng Jia, Xianpeng Lang, Xingang Wang, and Wenjun Mei. Recondreamer: Crafting world models for driving scene reconstruction via online restoration. *arXiv preprint arXiv:2411.19548*, 2024. 4
- [68] Dean A Pomerleau. Alvinn: An autonomous land vehicle in a neural network. *NeurIPS*, 1, 1988. 3
- [69] Aditya Prakash, Kashyap Chitta, and Andreas Geiger. Multi-modal fusion transformer for end-to-end autonomous driving. In *Conference on Computer Vision and Pattern Recognition (CVPR)*, 2021. 1, 3
- [70] Konstantinos Rematas, Andrew Liu, Pratul P. Srinivasan, Jonathan T. Barron, Andrea Tagliasacchi, Thomas Funkhouser, and Vittorio Ferrari. Urban radiance fields. *arXiv preprint arXiv:2111.14643*, 2021. 4
- [71] Katrin Renz, Kashyap Chitta, Otniel-Bogdan Mercea, A. Sophia Koepke, Zeynep Akata, and Andreas Geiger. Plant: explainable planning transformers via object-level representations. In *CoRL*, 2022. 3
- [72] Robin Rombach, Andreas Blattmann, Dominik Lorenz, Patrick Esser, and Björn Ommer. High-resolution image synthesis with latent diffusion models. In *Proceedings of the IEEE/CVF Conference on Computer Vision and Pattern Recognition (CVPR)*, pages 10684–10695, 2022. 8



- [73] Robin Rombach, Andreas Blattmann, Dominik Lorenz, Patrick Esser, and Björn Ommer. High-resolution image synthesis with latent diffusion models. *arXiv preprint arXiv:2112.10752*, 2022. 4
- [74] Stéphane Ross and Drew Bagnell. Efficient reductions for imitation learning. In *Proceedings of the thirteenth international conference on artificial intelligence and statistics*, pages 661–668. JMLR Workshop and Conference Proceedings, 2010. 5
- [75] Hao Shao, Letian Wang, RuoBing Chen, Hongsheng Li, and Yu Liu. Safety-enhanced autonomous driving using interpretable sensor fusion transformer. *CoRL*, 2022. 3
- [76] Hao Shao, Letian Wang, Ruobing Chen, Steven L Waslander, Hongsheng Li, and Yu Liu. Reasonnet: End-to-end driving with temporal and global reasoning. In *Proceedings of the IEEE/CVF Conference on Computer Vision and Pattern Recognition*, pages 13723–13733, 2023. 3
- [77] Jiaming Song, Chenlin Meng, and Stefano Ermon. Denoising diffusion implicit models. *arXiv preprint arXiv:2010.02502*, 2022. 3, 6
- [78] Haisheng Su, Wei Wu, and Junchi Yan. Difs: Ego-centric fully sparse paradigm with uncertainty denoising and iterative refinement for efficient end-to-end autonomous driving. *arXiv preprint arXiv:2409.09777*, 2024. 3
- [79] Wenchao Sun, Xuewu Lin, Yining Shi, Chuang Zhang, Haoran Wu, and Sifa Zheng. Sparsedrive: End-to-end autonomous driving via sparse scene representation. *arXiv preprint arXiv:2405.19620*, 2024. 3
- [80] Alexander Swerdlow, Runsheng Xu, and Bolei Zhou. Street-view image generation from a bird’s-eye view layout. *arXiv preprint arXiv:2301.04634*, 2024. 2, 4
- [81] Matthew Tancik, Vincent Casser, Xinchun Yan, Sabeek Pradhan, Ben Mildenhall, Pratul P. Srinivasan, Jonathan T. Barron, and Henrik Kretzschmar. Block-nerf: Scalable large scene neural view synthesis. *arXiv preprint arXiv:2202.05263*, 2022. 4
- [82] Qijian Tian, Xin Tan, Yuan Xie, and Lizhuang Ma. Drivingforward: Feed-forward 3d gaussian splatting for driving scene reconstruction from flexible surround-view input. *arXiv preprint arXiv:2409.12753*, 2024. 4
- [83] Martin Treiber, Ansgar Hennecke, and Dirk Helbing. Congested traffic states in empirical observations and microscopic simulations. *Physical Review E*, 62(2):1805–1824, 2000. 5
- [84] Dani Valevski, Yaniv Leviathan, Moab Arar, and Shlomi Fruchter. Diffusion models are real-time game engines. *arXiv preprint arXiv:2408.14837*, 2024. 6
- [85] Qitai Wang, Lue Fan, Yuqi Wang, Yuntao Chen, and Zhaoxiang Zhang. Freevs: Generative view synthesis on free driving trajectory. *arXiv preprint arXiv:2410.18079*, 2024. 4
- [86] Shihao Wang, Yingfei Liu, Tiancai Wang, Ying Li, and Xiangyu Zhang. Exploring object-centric temporal modeling for efficient multi-view 3d object detection. *arXiv preprint arXiv:2303.11926*, 2023. 8
- [87] Xiaofeng Wang, Zheng Zhu, Guan Huang, Xinze Chen, Jiagang Zhu, and Jiwen Lu. Drivedreamer: Towards real-world-driven world models for autonomous driving. *arXiv preprint arXiv:2309.09777*, 2023. 2, 3, 4, 6
- [88] Yuqi Wang, Jiawei He, Lue Fan, Hongxin Li, Yuntao Chen, and Zhaoxiang Zhang. Driving into the future: Multiview visual forecasting and planning with world model for autonomous driving. *arXiv preprint arXiv:2311.17918*, 2023. 2, 3, 4
- [89] Yuqing Wen, Yucheng Zhao, Yingfei Liu, Fan Jia, Yanhui Wang, Chong Luo, Chi Zhang, Tiancai Wang, Xiaoyan Sun, and Xiangyu Zhang. Panacea: Panoramic and controllable video generation for autonomous driving. *arXiv preprint arXiv:2311.16813*, 2023. 2, 4, 6, 8, 9
- [90] Yuqing Wen, Yucheng Zhao, Yingfei Liu, Binyuan Huang, Fan Jia, Yanhui Wang, Chi Zhang, Tiancai Wang, Xiaoyan Sun, and Xiangyu Zhang. Panacea+: Panoramic and controllable video generation for autonomous driving. *arXiv preprint arXiv:2408.07605*, 2024. 2, 3, 4, 8, 9
- [91] Xinchuo Weng, Boris Ivanovic, Yan Wang, Yue Wang, and Marco Pavone. Para-drive: Parallelized architecture for real-time autonomous driving. In *Proceedings of the IEEE/CVF Conference on Computer Vision and Pattern Recognition (CVPR)*, 2024. 1, 3
- [92] Penghao Wu, Xiaosong Jia, Li Chen, Junchi Yan, Hongyang Li, and Yu Qiao. Trajectory-guided control prediction for end-to-end autonomous driving: A simple yet strong baseline. In *NeurIPS*, 2022. 3
- [93] Penghao Wu, Li Chen, Hongyang Li, Xiaosong Jia, Junchi Yan, and Yu Qiao. Policy pre-training for autonomous driving via self-supervised geometric modeling. In *International Conference on Learning Representations*, 2023. 4
- [94] Wei Wu, Xi Guo, Weixuan Tang, Tingxuan Huang, Chiyu Wang, Dongyue Chen, and Chenjing Ding. Drivescape: Towards high-resolution controllable multi-view driving video generation. *arXiv preprint arXiv:2409.05463*, 2024. 3, 4
- [95] Wei Wu, Xi Guo, Weixuan Tang, Tingxuan Huang, Chiyu Wang, Dongyue Chen, and Chenjing Ding. Drivescape: Towards high-resolution controllable multi-view driving video generation. *arXiv preprint arXiv:2409.05463*, 2024. 4
- [96] Jinheng Xie, Yuexiang Li, Yawen Huang, Haozhe Liu, Wentian Zhang, Yefeng Zheng, and Mike Zheng Shou. Boxdiff: Text-to-image synthesis with training-free box-constrained diffusion. *arXiv preprint arXiv:2307.10816*, 2023. 4
- [97] Tianyi Yan, Dongming Wu, Wencheng Han, Junpeng Jiang, Xia Zhou, Kun Zhan, Cheng zhong Xu, and Jianbing Shen. Drivingsphere: Building a high-fidelity 4d world for closed-loop simulation. *arXiv preprint arXiv:2411.11252*, 2024. 4
- [98] Yunzhi Yan, Haotong Lin, Chenxu Zhou, Weijie Wang, Haiyang Sun, Kun Zhan, Xianpeng Lang, Xiaowei Zhou, and Sida Peng. Street gaussians: Modeling dynamic urban scenes with gaussian splatting. *arXiv preprint arXiv:2401.01339*, 2024. 4
- [99] Kairui Yang, Enhui Ma, Jibin Peng, Qing Guo, Di Lin, and Kaicheng Yu. Bevcontrol: Accurately controlling street-view elements with multi-perspective consistency via bev sketch layout. *arXiv preprint arXiv:2308.01661*, 2023. 2, 4, 8, 9

- [100] Xuemeng Yang, Licheng Wen, Yukai Ma, Jianbiao Mei, Xin Li, Tiantian Wei, Wenjie Lei, Daocheng Fu, Pinlong Cai, Min Dou, Botian Shi, Liang He, Yong Liu, and Yu Qiao. Drivearena: A closed-loop generative simulation platform for autonomous driving. *arXiv preprint arXiv:2408.00415*, 2024. 4
- [101] Ze Yang, Yun Chen, Jingkan Wang, Sivabalan Manivasagam, Wei-Chiu Ma, Anqi Joyce Yang, and Raquel Urtasun. Unisim: A neural closed-loop sensor simulator. *arXiv preprint arXiv:2308.01898*, 2023. 4
- [102] Zhenjie Yang, Xiaosong Jia, Hongyang Li, and Junchi Yan. Llm4drive: A survey of large language models for autonomous driving. In *NeurIPS 2024 Workshop on Open-World Agents*, 2023. 1
- [103] Zeyu Yang, Zijie Pan, Yuankun Yang, Xi Tian Zhu, and Li Zhang. Driving scene synthesis on free-form trajectories with generative prior. *arXiv preprint arXiv:2412.01717*, 2024. 4
- [104] Zhongrui Yu, Haoran Wang, Jinze Yang, Hanzhang Wang, Zeke Xie, Yunfeng Cai, Jiale Cao, Zhong Ji, and Mingming Sun. Sgd: Street view synthesis with gaussian splatting and diffusion prior. *arXiv preprint arXiv:2403.20079*, 2024. 4
- [105] Jiang-Tian Zhai, Ze Feng, Jinhao Du, Yongqiang Mao, Jiang-Jiang Liu, Zichang Tan, Yifu Zhang, Xiaoqing Ye, and Jingdong Wang. Rethinking the open-loop evaluation of end-to-end autonomous driving in nuscenes. *arXiv preprint arXiv:2305.10430*, 2023. 1, 3, 10
- [106] Diankun Zhang, Guoan Wang, Runwen Zhu, Jianbo Zhao, Xiwu Chen, Siyu Zhang, Jiahao Gong, Qibin Zhou, Wenyuan Zhang, Ningzi Wang, Feiyang Tan, Hangning Zhou, Ziyao Xu, Haotian Yao, Chi Zhang, Xiaojun Liu, Xiaoguang Di, and Bin Li. Sparsead: Sparse query-centric paradigm for efficient end-to-end autonomous driving. *arXiv preprint arXiv:2404.06892*, 2024. 3
- [107] Jinhua Zhang, Hualian Sheng, Sijia Cai, Bing Deng, Qiao Liang, Wen Li, Ying Fu, Jieping Ye, and Shuhang Gu. Perldiff: Controllable street view synthesis using perspective-layout diffusion models. *arXiv preprint arXiv:2407.06109*, 2024. 4
- [108] Lvmin Zhang, Anyi Rao, and Maneesh Agrawala. Adding conditional control to text-to-image diffusion models. *arXiv preprint arXiv:2302.05543*, 2023. 2, 3, 4, 5
- [109] Qingwen Zhang, Mingkai Tang, Ruoyu Geng, Feiyi Chen, Ren Xin, and Lujia Wang. Mmfn: multi-modal-fusion-net for end-to-end driving. *IRIS*, 2022. 3
- [110] Yumeng Zhang, Shi Gong, Kaixin Xiong, Xiaoqing Ye, Xiao Tan, Fan Wang, Jizhou Huang, Hua Wu, and Haifeng Wang. Bevworld: A multimodal world model for autonomous driving via unified bev latent space. *arXiv preprint arXiv:2407.05679*, 2024. 3
- [111] Zhejun Zhang, Alexander Liniger, Dengxin Dai, Fisher Yu, and Luc Van Gool. End-to-end urban driving by imitating a reinforcement learning coach. In *ICCV*, 2021. 3
- [112] Guosheng Zhao, Chaojun Ni, Xiaofeng Wang, Zheng Zhu, Xueyang Zhang, Yida Wang, Guan Huang, Xinze Chen, Boyuan Wang, Youyi Zhang, Wenjun Mei, and Xingang Wang. Drivedreamer4d: World models are effective data machines for 4d driving scene representation. *arXiv preprint arXiv:2410.13571*, 2024. 4
- [113] Guosheng Zhao, Xiaofeng Wang, Zheng Zhu, Xinze Chen, Guan Huang, Xiaoyi Bao, and Xingang Wang. Drivedreamer-2: Llm-enhanced world models for diverse driving video generation. *arXiv preprint arXiv:2403.06845*, 2024. 2, 3, 4
- [114] Wenliang Zhao, Lujia Bai, Yongming Rao, Jie Zhou, and Jiwen Lu. Unipc: A unified predictor-corrector framework for fast sampling of diffusion models. *arXiv preprint arXiv:2302.04867*, 2023. 8
- [115] Hongyu Zhou, Longzhong Lin, Jiabao Wang, Yichong Lu, Dongfeng Bai, Bingbing Liu, Yue Wang, Andreas Geiger, and Yiyi Liao. Hugsim: A real-time, photo-realistic and closed-loop simulator for autonomous driving. *arXiv preprint arXiv:2412.01718*, 2024. 4
- [116] Xiaoyu Zhou, Zhiwei Lin, Xiaojun Shan, Yongtao Wang, Deqing Sun, and Ming-Hsuan Yang. Driving-gaussian: Composite gaussian splatting for surrounding dynamic autonomous driving scenes. *arXiv preprint arXiv:2312.07920*, 2024. 4
- [117] Yunsong Zhou, Michael Simon, Zhenghao Peng, Sicheng Mo, Hongzi Zhu, Minyi Guo, and Bolei Zhou. Simgen: Simulator-conditioned driving scene generation. *arXiv preprint arXiv:2406.09386*, 2024. 4
- [118] Yutao Zhu, Xiaosong Jia, Xinyu Yang, and Junchi Yan. Flatfusion: Delving into details of sparse transformer-based camera-lidar fusion for autonomous driving. *arXiv preprint arXiv:2408.06832*, 2024. 4